Technische Universiteit
Eindhoven
University of Technology

Department of Mechanical Engineering

Advanced motion control (4CM60)

Exercise set 2

Student name:	**Student ID:**
Tom van de Laar	1265938
Job Meijer	1268155

Version 1

Eindhoven, May 2019

1 Exercise 2.6

a) Computing the poles and zeros of $G_a(s)$:

$$G_a(s) = \frac{1}{(s+1)(s+2)} \begin{bmatrix} 1 & -1 \\ s^2+s-4 & 2s^2-s-8 \\ s^2-4 & 2s^2-8 \end{bmatrix}$$

The minors of order 1 are all the non-zero values of $G_a(s)$. Because there are no non-zero transfer functions in $G_a(s)$, all elements of this matrix are first order minors. The minors of order 2 are determined by computing the determinant three times, each time with another row of $G_a(s)$ removed. This results in:

$$M_1 = det \begin{bmatrix} \frac{s^2+s-4}{(s+1)(s+2)} & \frac{2s^2-s-8}{(s+1)(s+2)} \\ \frac{s^{-4}}{(s+1)(s+2)} & \frac{2s^2-8}{(s+1)(s+2)} \end{bmatrix} = \frac{3s(s-2)(s+2)}{((s+1)(s+2))^2} = \frac{3s(s-2)}{((s+1)^2(s+2))}$$

$$M_2 = det \begin{bmatrix} \frac{1}{(s+1)(s+2)} & \frac{-1}{(s+1)(s+2)} \\ \frac{s^{-}4}{(s+1)(s+2)} & \frac{2s^2-8}{(s+1)(s+2)} \end{bmatrix} = \frac{3(s-2)(s+2)}{((s+1)(s+2))^2} = \frac{3(s-2)}{((s+1)^2(s+2))}$$

$$M_3 = det \begin{bmatrix} \frac{1}{(s+1)(s+2)} & \frac{-1}{(s+1)(s+2)} \\ \frac{s^2+s-4}{(s+1)(s+2)} & \frac{2s^2-s-8}{(s+1)(s+2)} \end{bmatrix} = \frac{3(s-2)(s+2)}{((s+1)(s+2))^2} = \frac{3(s-2)}{((s+1)^2(s+2))}$$

Now determining the least common denominator results in $\phi(s) = (s+2)(s+1)^2$, therefore the system has three poles: one at -2 and two at -1. The zeros of the system are determined by the common factor of all second order minors, which is $(s-2)$ resulting in one zero at 2.

b) Computing the poles and zeros of $G_b(s)$:

$$G_b(s) = \begin{bmatrix} \frac{s+2}{s} & \frac{-1}{2(s+1)} \\ \frac{(s+1)(s+2)}{s^2} & \frac{1}{2s} \end{bmatrix}$$

Again, the first order minors are determined by taking all non-zero values from $G_b(s)$ and the second order minor is determined by computing the determinant of $G_b(s)$:

$$M = det \begin{bmatrix} \frac{s+2}{s} & \frac{-1}{2(s+1)} \\ \frac{(s+1)(s+2)}{s^2} & \frac{1}{2s} \end{bmatrix} = \frac{s+2}{s^2}$$

The least common denominator from the first order minors is $(s+1)$ and the least common denominator from the second order minor is s^2. This results in $\phi(s) = s^2(s+1)$, indicating that the system has two poles at 0 and one at -1.

Because there now is only one second order minor, to determine the zeros of the system the following equation is solved:
$\frac{n(s)}{\phi(s)} = M \longrightarrow \frac{n(s)}{s^2(s+1)} = \frac{s+2}{s^2} \longrightarrow n(s) = (s+1)(s+2)$, indicating that the zeros of the system are -1 and -2.

2 Exercise 2.7

The open-loop transfer function matrix is given as:

$$L(s) = \begin{bmatrix} \frac{s+10}{s^2+s+10} & \frac{10}{s^4+s^3+10s^2+s+1} \\ \frac{\alpha}{s^2+0.1s+10} & \frac{s+10}{0.1s^2+s+10} \end{bmatrix} \tag{2.1}$$

Where $\alpha \in [0, 10]$. To conclude about stability of the system the closed-loop poles are calculated as well as the characteristic loci. A MIMO system can considered to be stable iff the characteristic loci has P anti-clockwise encirclements of the origin and does not pas trough the origin. Where, P is the number of unstable poles in L(s). Moreover, the characteristic loci is taken together by $\prod_i (1 + \lambda_i(L(s))$ and the closed-loop poles are calculated using $L(s) \cdot (I + L(s))^{-1}$. The results can be found in figure 2.1. For $\alpha = 4$ one of the closed-loop poles lies on the boundary of stability. For a higher α the system has RHP closed-loop poles and is therefore unstable. For the characteristic loci analysis the open-loop poles are computed, however they are never in the RHP ($P = 0$). After $\alpha = 4$ the characteristic loci contains a clockwise encirclement which can be seen in figure 2.1a. Therefore the closed-loop system becomes unstable for $\alpha \geq 4$. If $\alpha = 0$ the characteristic loci gives the same result as the in depended SISO nyquists of the diagonals. This has to do with the fact that if the one term of the off diagonal is zero only the diagonal terms are used as eigenvalues.

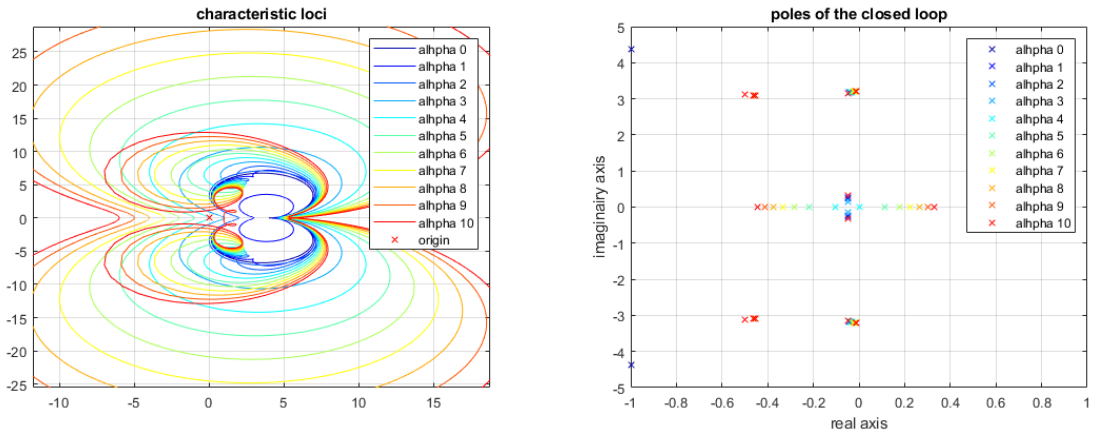

(a) Characteristic loci

(b) Closed-loop poles

Figure 2.1: Stability with nyquist

3 Exercise 2.8

a) The given set of linear equations: $y = Ax$ where $y \in \mathbf{R}^l$, $x \in \mathbf{R}^m$ and $A \in \mathbf{R}^{l \times m}$. Assumed is that $r = l \leq m$ where r is the rank of A.

The solution x to $y = Ax$ that minimizes $\|x\|_2$ is the solution to $y = A^\dagger x$. Because $r = l \leq m$, A has full row rank resulting in an infinite number of solutions to $y = Ax$. The solution that minimizes $\|x\|_2$ is $A^\dagger = A^H(AA^H)^{-1}$, resulting in the right inverse of A.

b) Again the system $y = Ax$ from a is considered but now with $r = m \leq l$ where r is the rank of A. The solution for x that minimizes $\|y - Ax\|_2$ is computed by $A^\dagger = (A^H A)^{-1}A^H$, resulting in the left inverse of A.

c) A rigid-body decoupling of the system G is performed at the frequency where the system behaves predominantly as a rigid-body, the lowest frequency from the measurement data: 0.1 rad/s. This is done by determining the matrices T_u and T_y such that $G_{dec}(s) = T_y G(s) T_u$.

Determining T_y is done by creating a matrix that transforms the outputs of $G(s)$ to the outputs of $G_{dec}(s)$. This results in:

$$T_y = \begin{bmatrix} 1 & 0 & 0 & 0 & 0 & 0 \\ 0 & 1 & 0 & 0 & 0 & 0 \\ 0 & 0 & 0.25 & 0.25 & 0.25 & 0.25 \end{bmatrix}$$

Now T_u is determined using the following equation: $T_u = (T_y G(0.1))^{-1}$. Here $G(0.1)$ is chosen because this is the lowest measured frequency, where the system behaves predominantly as a rigid-body. Because the frequency is almost 0, the used decoupling method is steady-state decoupling. Also the Moore-Penrose inverse used because the matrix $T_y G(0.1)$ is not square. This results in the decoupled system $G_{dec}(s) = T_y G(s) T_u$ which is shown in Figure 3.1.

Determining a solution that minimizes the actuator forces in terms of the 2-norm is done by decoupling the system in steady state, resulting in a lower gain at higher frequencies. This results in a minimized actuator force since the average of the open-loop bode is lower. Steady-state decoupling also reduces the noise for the same reason: a lower average gain.

To determine a solution that minimizes the 2-norm of the following residual:

$$\begin{bmatrix} x_1 \\ y_1 \\ z_1 \\ z_2 \\ z_3 \\ z_4 \end{bmatrix} - A \begin{bmatrix} x \\ y \\ z \end{bmatrix}$$

By taking $A = T_y^T$ the result after subtraction is only the noise from the sensors z_1 to z_4. Because this noise is independent and normally distributed, its average is zero. A 2-norm

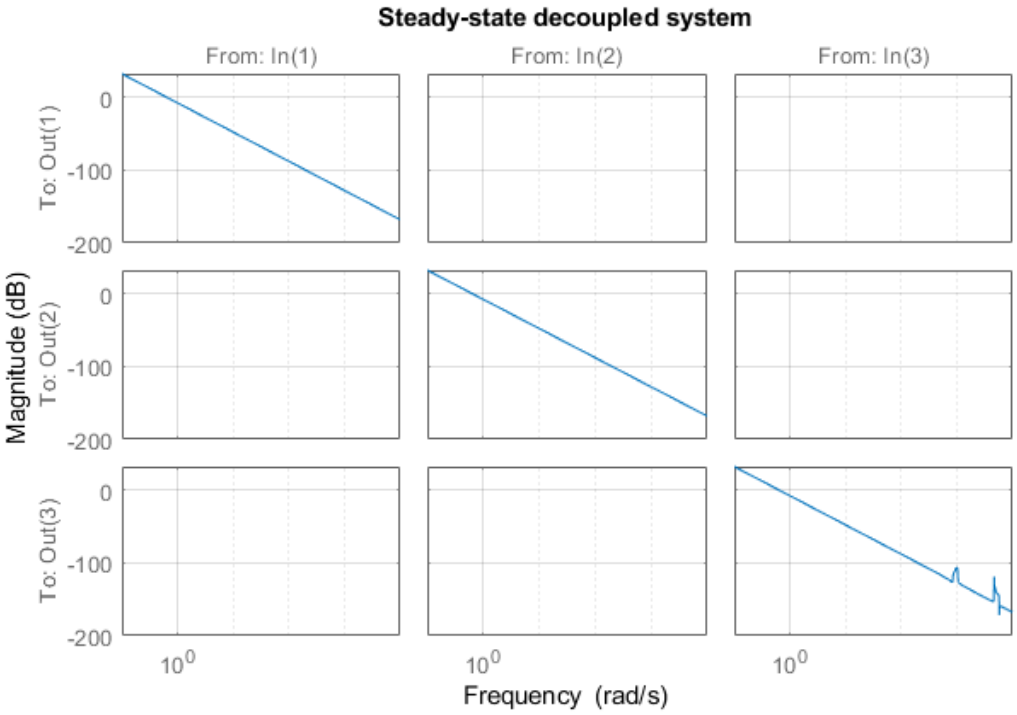

Figure 3.1: Steady-state decoupled system

is computing an average, so in steady state this results in the minimal 2-norm of the residuals.

d) Now a decentralized controller K_1 for the decoupled system is designed in order to control it in the x, y and z directions with a cross-over frequency of $80Hz$, closed-loop stability and 'good' low-frequent disturbance attenuation.

The decoupled system exists of three second order integrators. To get a stable system, a lead filter is added around the desired cross-over frequency:
$Filter(s) = \dfrac{\frac{1}{2\pi f_1}s + 1}{\frac{1}{2\pi f_2}s + 1}$ where $f_1 = 20Hz$ and $f_2 = \dfrac{f_c^2}{f_1}$. The value for $f1$ is chosen to obtain a phase lead of ≈ 60 degrees around the desired cross-over frequency to achieve balance between response time and overshoot.

Now the needed gain is determined to get the desired cross-over frequency. With the current decoupled system $Filter(s) \cdot G_{dec}(s)$ the open-loop gain at the desired cross-over frequency is -104 dB. To obtain the desired cross-over frequency, the gain of controller K_1 is set to $10^{(\frac{104}{20})} \approx 158,000$.

Because the loops are perfectly decoupled, it is possible to verify the stability of the system using standard Nyquist diagrams. In Figure 3.2 are the Nyquist diagrams shown for all three separate loops, which all have enough margin from the -1 point on the real axis.

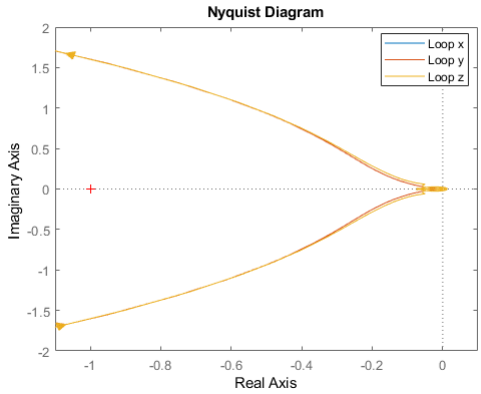

Figure 3.2: Nyquist diagram of the system with controller $K_1(s)$

The cross over frequency is validated by the open-loop response of the three separate loops which are shown in Figure 3.3. The low-frequency disturbance attenuation is validated by the sensitivities of the three loops shown in Figure 3.4.

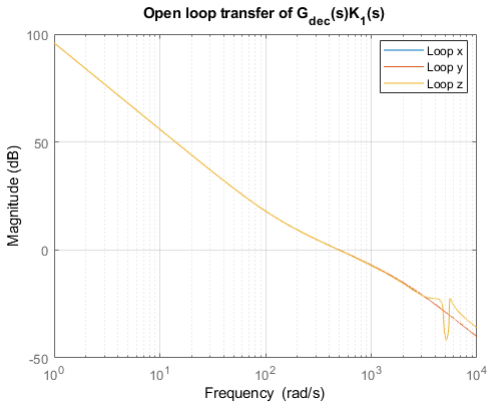

Figure 3.3: Open-loop response of the system with controller $K_1(s)$

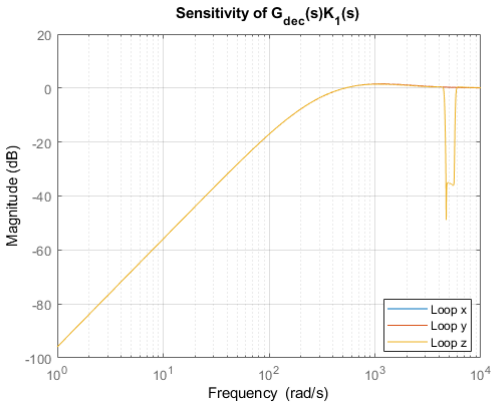

Figure 3.4: Sensitivity of the system with controller $K_1(s)$

e) Controller K_2 is now designed just as in exercise 8d, however now the desired cross-over frequency is 220 Hz. To obtain a phase lead of 60 degrees at 220 Hz, f_1 is now set to 60 Hz and f_c to 220 Hz. The gain is also increased to $1,131,400$.

With this higher cross-over frequency a peak is visible at the gain of the decoupled z axis, which is just below 0 dB. At this peak the phase jumps +360 degrees. The closed-loop system is stable as can be derived from the Nyquist diagram of Figure 3.5. From Figure 3.6 can be verified that the system has a cross-over frequency of 220 Hz. Because of the resonance peak in the z axis loop the margins of the system are much lower compared to controller $K_1(s)$.

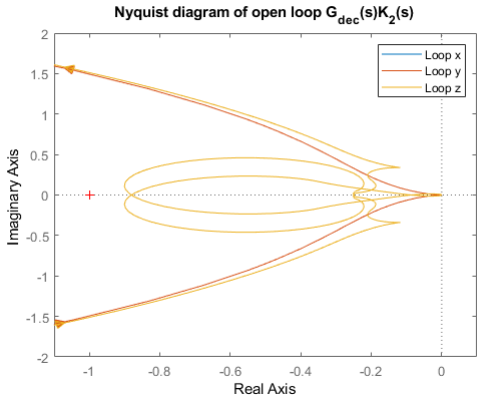

Figure 3.5: Nyquist diagram of the system with controller $K_2(s)$

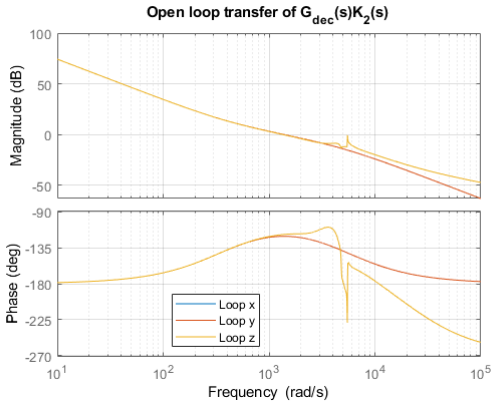

Figure 3.6: Open-loop response of the system with controller $K_2(s)$

f) Because from the Bode plot in Figure 3.1 can be concluded that the system has flexible dynamic behavior. A modal analysis is performed on the system resulting in the following modal matrix:

$$\Phi = [\phi_1 \phi_2 \phi_3] = \begin{bmatrix} 1 & -0.4 & -0.7 \\ 1 & 0.15 & -0.09 \\ 1 & 0.15 & 0.14 \\ 1 & -0.4 & 0.62 \end{bmatrix}$$

Now the z axis is divided in a rigid body mode z_{rb} and two flexible modes: z_{flex1} and z_{flex2}, resulting in the following system:

$$\begin{bmatrix} x \\ y \\ z_{rb} \\ z_{flex1} \\ z_{flex2} \end{bmatrix} = T_{y2} G T_{u2} \begin{bmatrix} F_x \\ F_y \\ F_{rb} \\ F_{flex1} \\ F_{flex2} \end{bmatrix}$$

To determine T_{y2}, the relation between the output of G and the new desired output is determined. The relation between the in- and output for the x and y axis is unchanged compared to exercise 8c, where it was a gain of 1. For the z axis the given modal matrix is used, which is inverted to obtain the relation from G to y. Because this matrix is not square, the Moore-Penrose inverse is used. This resulted in:

$$T_{y2} = \begin{bmatrix} 1 & 0 & 0 & 0 & 0 & 0 \\ 0 & 1 & 0 & 0 & 0 & 0 \\ 0 & 0 & 0.1417 & 0.3646 & 0.3627 & 0.1310 \\ 0 & 0 & -0.8222 & 0.9242 & 0.8940 & -0.9960 \\ 0 & 0 & -0.7353 & -0.1281 & 0.1281 & 0.7353 \end{bmatrix}$$

Now T_{u2} is determined by taking the Moore-Penrose inverse of $T_{y2} \cdot G(0.1)$, the same method as in exercise 8c. The Bode plot of the decoupled system is shown in Figure 3.7.

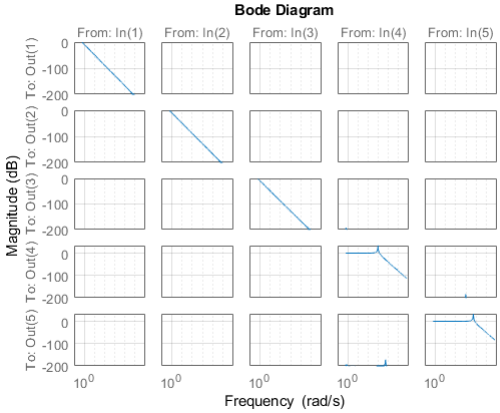

Figure 3.7: Decoupled system with z_{rb}, z_{flex1} and z_{flex2}

g) A controller is created for the system $G_{modal}(s)$ to achieve a bandwidth of 220 Hz for the x, y and z_{rb} loops. Because these loops now all have the same frequency response, the control strategy for them is the same: adding a lead filter at the desired cross-over frequency to obtain a phase margin of ≈ 60 degrees and increasing the gain until the cross-over frequency is reached. The two flexible modes need to be stable first, which is done by adding a lead filter to get gain margin at the cross-over frequency. This results in the same controller as for the system in exercise 8e.

for the two flexible modes, two separate controllers are designed because they both have their resonance peak at a different frequency: 150 and 820 Hz. The controllers used for the flexible mode also consist of a lead filter and a gain. The lead filter is used to stabilize the two loops by adding phase at the cross-over frequency and the gain is used to reduce the sensitivity at lower frequencies where the point to be controlled is actuated at. The open-loop response is shown in Figure 3.9 and the Nyquist plot is shown in Figure 3.8.

h) Now is assumed that one of the designed controllers $K_1(s)$, $K_2(s)$ and K_{modal} is implemented on $G(s)$ instead of $T_y G T_u$ or $T_{y2} G T_{u2}$. These controllers are K_1^{org}, K_2^{org} and K_{modal}^{org}

$$K_1^{org} = \begin{bmatrix} XK_{1(1,1)} & XK_{1(1,1)} & 0 & 0 & 0 & 0 & 0 & 0 \\ 0 & 0 & XK_{1(2,2)} & XK_{1(2,2)} & 0 & 0 & 0 & 0 \\ 0 & 0 & 0 & 0 & K_{1(3,3)} & K_{1(3,3)} & K_{1(3,3)} & K_{1(3,3)} \\ 0 & 0 & 0 & 0 & K_{1(3,3)} & K_{1(3,3)} & K_{1(3,3)} & K_{1(3,3)} \\ 0 & 0 & 0 & 0 & K_{1(3,3)} & K_{1(3,3)} & K_{1(3,3)} & K_{1(3,3)} \\ 0 & 0 & 0 & 0 & K_{1(3,3)} & K_{1(3,3)} & K_{1(3,3)} & K_{1(3,3)} \end{bmatrix}$$

$$K_2^{org} = \begin{bmatrix} XK_{2(1,1)} & XK_{2(1,1)} & 0 & 0 & 0 & 0 & 0 & 0 \\ 0 & 0 & XK_{2(2,2)} & XK_{2(2,2)} & 0 & 0 & 0 & 0 \\ 0 & 0 & 0 & 0 & K_{2(3,3)} & K_{2(3,3)} & K_{2(3,3)} & K_{2(3,3)} \\ 0 & 0 & 0 & 0 & K_{2(3,3)} & K_{2(3,3)} & K_{2(3,3)} & K_{2(3,3)} \\ 0 & 0 & 0 & 0 & K_{2(3,3)} & K_{2(3,3)} & K_{2(3,3)} & K_{2(3,3)} \\ 0 & 0 & 0 & 0 & K_{2(3,3)} & K_{2(3,3)} & K_{2(3,3)} & K_{2(3,3)} \end{bmatrix}$$

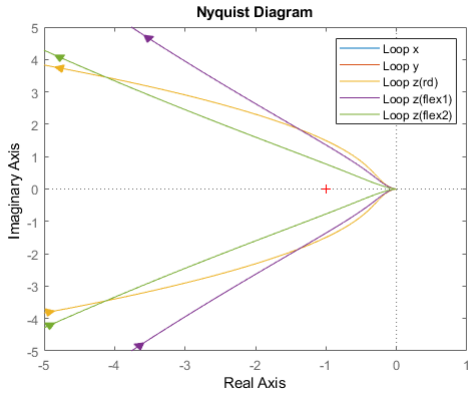

Figure 3.8: Nyquist diagram of the system with controller $K_{modal}(s)$

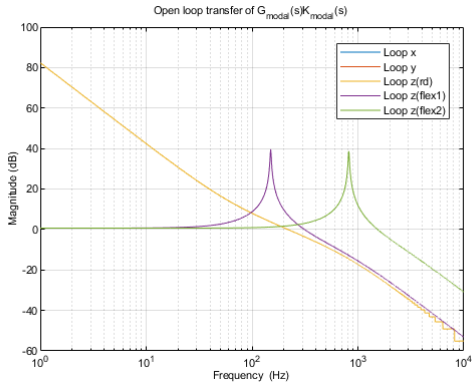

Figure 3.9: Open-loop response of the system with controller $K_{modal}(s)$

$$K_{modal}^{org} = \begin{bmatrix} XK_{modal(1,1)} & XK_{modal(1,1)} & 0 & 0 & 0 & 0 & 0 \\ 0 & 0 & XK_{modal(2,2)} & XK_{modal(2,2)} & 0 & 0 & 0 \\ 0 & 0 & 0 & 0 & K_{modal(3,3)} & K_{modal(3,3)} & K_{modal(3,3)} \\ 0 & 0 & 0 & 0 & K_{modal(3,3)} & K_{modal(3,3)} & K_{modal(3,3)} \\ 0 & 0 & 0 & 0 & K_{modal(3,3)} & K_{modal(3,3)} & K_{modal(3,3)} \\ 0 & 0 & 0 & 0 & K_{modal(3,3)} & K_{modal(3,3)} & K_{modal(3,3)} \end{bmatrix}$$

where $X = \dfrac{32}{20}$.

These controllers are diagonal and their McMillan degree is 1 for K_1^{org}, K_2^{org} and K_{modal}^{org} since they all have one unique pole on across the diagonal.
The chosen controller to implement is $K_1(s)$, because this enables the possibility to keep the peaks of the resonance modes of the z axis below 0 dB.

i) Now a sinusoidal output disturbance is present at sensor z_3, affecting the measured variable before the sensor reading is performed. The transfer function that quantifies the disturbance attenuation properties from this output disturbance to the sensor z_3 is the transfer of F_{z3} to z_3. This transfer function is:

$$\frac{z_3(s)}{F_{z3}(s)} = \frac{-0.0002831s^3 - 0.6913s^2 + 411.9s + 7.706e06}{s^4 + 1236s^3 + 2.312e07s^2}.$$

This transfer function has a high gain at low frequencies. Since the controllers are designed with a low sensitivity at frequencies up to 200 Hz, these disturbances are cancelled.

4 Exercise 2.9

a) In this exercise a controller is designed that suppresses vibrations of the system by keeping y constant. The requirements for the controller are:
- Sensitivity below 0 dB between 1 and 10 Hz
- Modulus margin ¡ 6 dB
- Closed loop transfer function ¡ -30 dB for frequencies above 100 Hz

This is achieved by implementing a controller with a lowpass and a highpass filter, resulting in $K(s) = K_{lowpass}(s) \cdot K_{highpass}$. The values for this filter are determined manually and the transfer functions are:
- Lowpass filter: $K_{lowpass}(s) = \dfrac{1}{s + 4\pi}$
- Highpass filter: $K_{highpass}(s) = \dfrac{s + 4.6\pi}{1}$

The sensitivity is shown in Figure 4.1 and the closed-loop response is shown in Figure 4.2. From the sensitivity can be concluded that the first two requirements are achieved, because it is below 0 dB between 1 and 10 Hz and always below 6 dB. From the closed-loop response can be concluded that it is below -30 dB for frequencies of 100 Hz and up.

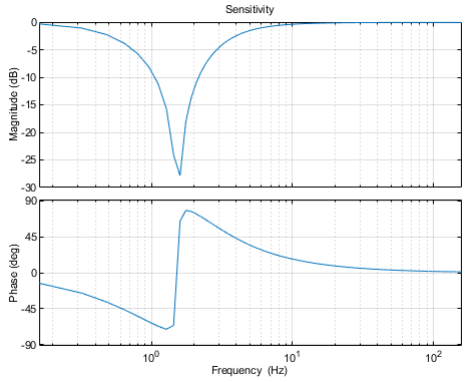

Figure 4.1: Sensitivity

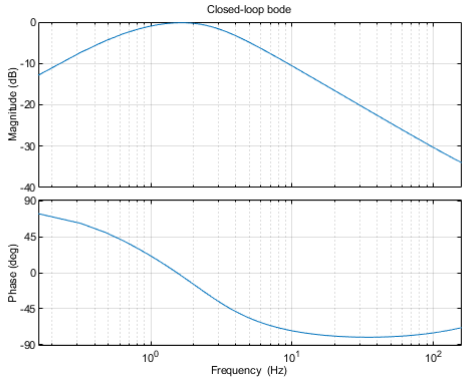

Figure 4.2: Closed loop

b) Now is determined if the true system $G_{frf}(s)$ is stable when controller $K(s)$ is implemented on it.

There are three tests that determine if the system is stable based on $E(s)$ and $T_{mod}(s)$:
- $E(s) = (G_{frf}(s) - G_{mod}(s))G_{mod}^{-1}(s)$ which indicates the error between $G_{frf}(s)$ and $G_{mod}(s)$.
- $T_{mod}(s) = \dfrac{G_{mod}(s)K(s)}{1 + G_{mod}(s)K(s)}$ which is the closed-loop response of $G_{mod}(s)$.

1. iff $det(I + E(s)T_{mod}(s)$ does not encircle the origin as ω traverses the Nyquist D-contour.
2. point 1 is satisfied if $\rho(E(j\omega)T_{mod}(j\omega)) < 1 \forall \omega$
3. point 2 is satisfied if $\overline{\sigma}(T_{mod}(j\omega) < \mu_{T_{mod}}^{-1}(E(j\omega)), \forall \omega$

If test 3 is satisfied, test 1 and 2 are also satisfied. The value for $\overline{\sigma}(T_{mod}(j\omega)$ is computed by doing an SVD of $T_{mod}(j\omega)$ and $\mu^{-1}_{T_{mod}}(E(j\omega))$ is computed from $|E(j\omega)|^{-1}$. This results in Figure 4.3. From this figure can be concluded that the system G_{frf} is not stable with controller K since $\overline{\sigma}(T_{mod}(j\omega) < \mu^{-1}_{T_{mod}}(E(j\omega))$ does not hold $\forall\omega$, so stability can not be guaranteed.

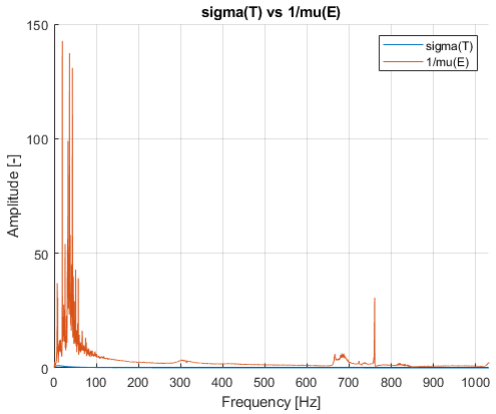

Figure 4.3: $T_{mod}(j\omega)$ $and\mu^{-1}_{T_{mod}}(E(j\omega))$

c) Redesigning the controller go guarantee stability for both G_{mod} and G_{frf} resulted in the following controller adjustments: a lead filter is added at low frequencies in order to reduce the gain of the open-loop and sensitivity at these frequencies. This is done because the G_{frf} data showed a much larger amplitude compared to G_{mod}. The transfer function of this lead filter is $\dfrac{s+0.01\pi}{s+8\pi}$.

d) Evaluating the performance of the designed controller on the model G_{mod} by applying an input disturbance d_1. The response of the open-loop and closed-loop system for a sinusoidal disturbance of 0.1, 2 and 20 Hz are determined. Since the disturbance acts directly on the mass, it has the same behavior as an input. Therefor the sensitivity is used to determine the behavior of the output based on the disturbance. At 0.1 and 20 Hz, the sensitivity is about 1. This indicates that there is no big difference between the open- and closed-loop system. At 2 Hz however there is a dip in the sensitivity, indicating that the closed-loop system will cancel out the disturbance much better compared to the open-loop situation at that frequency.

e) Redesigning the controller to enhance disturbance attenuation properties at 20 Hz, while retaining approximately similar disturbance attenuation at 0.1 and 2 Hz. To get this result, the controller is adjusted while keeping an eye on the sensitivity. The gain of the sensitivity function should be decreased at 20 Hz to achieve the desired result. This is achieved by adding a lead filter with the following transfer function: $\dfrac{s+8\pi}{s+50\pi}$, determined after manual tuning. This resulted in $-0.5dB$ of extra disturbance attenuation at 20 Hz, while not chaning the disturbance attenuation at 0.1 Hz.

f) Now is assumed that an output disturbance is present. It is predicted that the controller design of exercise c is optimistic at higher frequencies and pessimistic in predicting the output disturbance rejection properties of the true system G_{frf} at lower frequencies. This is based on the sensitivity of G_{frf} and G_{mod}, which has the biggest difference at low frequencies.

5 Exercise 2.10

a) A decenteralized controller K is designed based on the diagonal frequency response function measurement G_d. The following requirements are taken into account:
- The closed-loop system is stable and has a modulus margin of $< 6dB$
- The disturbance attenuation for low frequencies is determined by the sensitivity, that should be $< 0dB$ for frequencies below f_{bb}

The inputs 1, 2 and 4 are respectively the inputs of the x, y and z axis. Inputs 3, 5 and 6 are the rotation inputs of the x, y and z axis.

Started on the Exercise but could not be finished before deadline

6 Exercise 2.11

Started on the Exercise but could not be finished before deadline

7 Exercise 2.12

a) By combining G(s) and K(s), L(s) is formed in equation 9.1. Stability of the diagonal loops is determined by applying nyquist to $L(s)$. A loop is considered to be stable when the nyquist plot makes -P clockwise encirclements around -1, where P is number of open-loop RHP poles. Both of the diagonal loop contain no open-loop RHP poles, so no clockwise encirclements are needed. Therefore, the diagonal loops are considered to be stable, figure 7.1 shows the diagonal nyquist plots.

$$G = \begin{bmatrix} \frac{1}{s+1} & \frac{1}{s-2} \\ 0 & \frac{1}{s+3} \end{bmatrix} \tag{7.1}$$

$$K = \begin{bmatrix} 4 & 0 \\ 0 & 4 \end{bmatrix} \tag{7.2}$$

$$L = \begin{bmatrix} \frac{4}{s+1} & \frac{4}{s-2} \\ 0 & \frac{4}{s+3} \end{bmatrix} \tag{7.3}$$

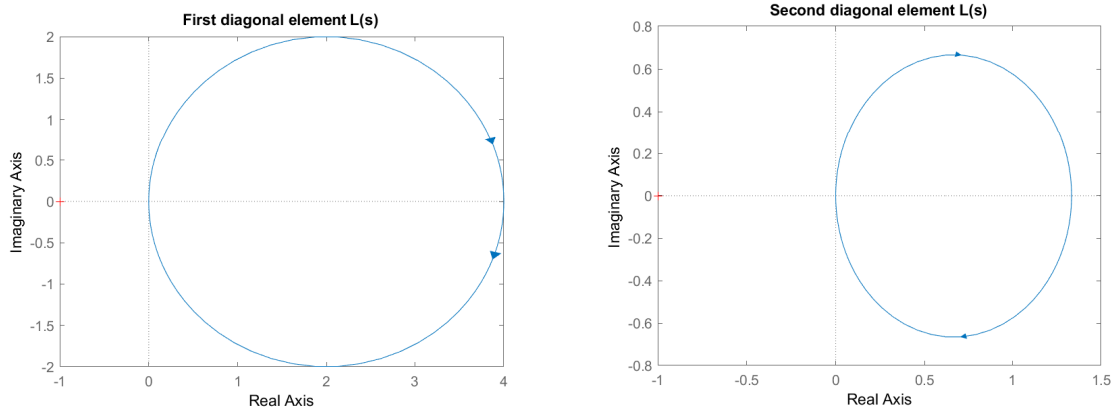

(a) First element of L(s)

(b) Second element of L(s)

Figure 7.1: Diagonal nyquist of L(s)

Furthermore, the characteristic loci ($\lambda_i(L(j\omega))$ is determined to conclude about stability. The characteristic loci is calculated using $det[\lambda(s)I - L(s)] = 0$. This results in $(\lambda(s) - \frac{4}{s+1})(\lambda(s) - \frac{4}{s+3}) = 0$. This finally leads to $\lambda_1(s) = \frac{4}{s+1}$ and $\lambda_2(s) = \frac{4}{s+3}$. When s is replaced by $j\omega$ the characteristic loci can be plotted, results in figure 7.2. The Loci is identical to the diagonal nyquist because one of the off diagonal terms is zero and therefore only the diagonal terms have effect on the eigenvalues. The closed-loop system is unstable because the loci makes no clockwise encirclements. However, G contains one RHP pole in open-loop. Therefore, the loci should make at least one clockwise encirclement.

b) The closed loop system L is considered, equation 7.4. The eigenvalues are computed by hand. $det[\lambda(s)I - L(s)] = 0$ is used to calculated the eigenvalues.

$$L(s) = \begin{bmatrix} \frac{1}{s+1} & 1 \\ \frac{s-1}{s+1} & 1 \end{bmatrix} \tag{7.4}$$

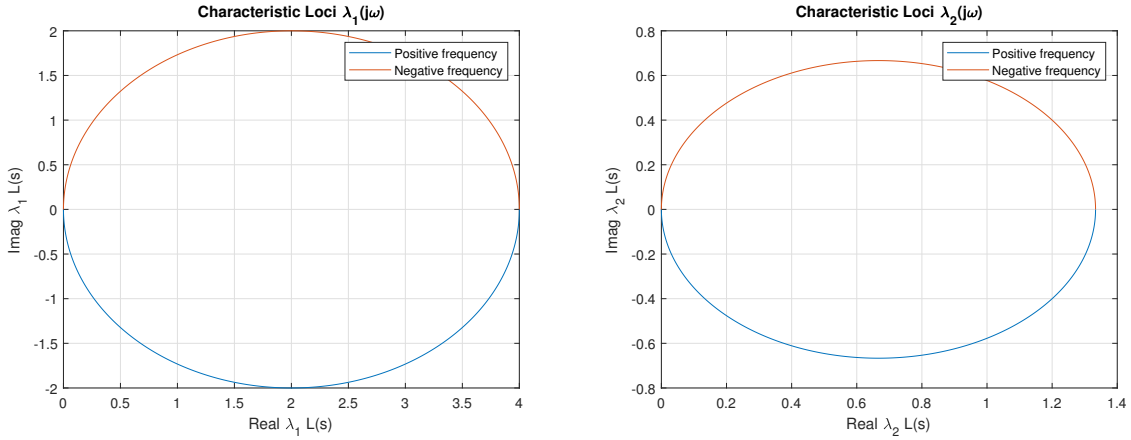

(a) λ_1 of L(s)

(b) λ_2 of L(s)

Figure 7.2: Characteristic loci of L(s)

$$(\lambda(s) - \tfrac{1}{s+1})(\lambda(s) - 1) - (\tfrac{s-1}{s+1}) = 0 \tag{7.5}$$

Which eventualy results in the eigenvalues:

$$\lambda_1(s) = \frac{-s + \sqrt{5s^2 + 4s}}{2(s+1)} \tag{7.6}$$

$$\lambda_2(s) = \frac{-s - \sqrt{5s^2 + 4s}}{2(s+1)} \tag{7.7}$$

From figure 7.3 can be concluded that the system is unstable in closed loop. The spectral radius stability condition is used here fore. The proof of this theorem is based on the generalized Nyquist theorem. Moreover, the det(I + L(s)) used in this theorem encircle the origin for an eigenvalue greater then one. In figure 7.3b the eigenvalue crosses the unit circle and is therefore unstable.

Theorem 4.11 Spectral radius stability condition. *Consider a system with a stable loop transfer function L(s) Then the closed-loop system is stable if*

$$\rho(L(j\omega) < 1 \quad \forall\omega \tag{7.8}$$

c.a) The system with open loop gain $L(s) = \frac{(s+1)^2}{s^3}$ is considered. The open loop can become unstable if for instance a step input is applied. The poles of the open loop gain L(S) are on top of the imaginary axis. According to the nyquist theorem these poles are excluded from counting RHP poles. Therefore, it is not necessary to make any anti-clockwise encirclements in the nyquist plot. However, the nyquist makes one anti-clockwise encirclement. Moreover, the closed loop is thereby considered to be stable.

c.b) The system with open loop gain $L(s) = \begin{bmatrix} \frac{1}{s+1} & \frac{1}{s^3} \\ 0 & \frac{1}{s+2} \end{bmatrix}$ is now considered. The open-loop pole polynomial is equal to $\phi_{ol} = (s+1)(s+2)s^3$. This system can become open-loop unstable when a step input is applied to the second input. The pole polynomial has poles on

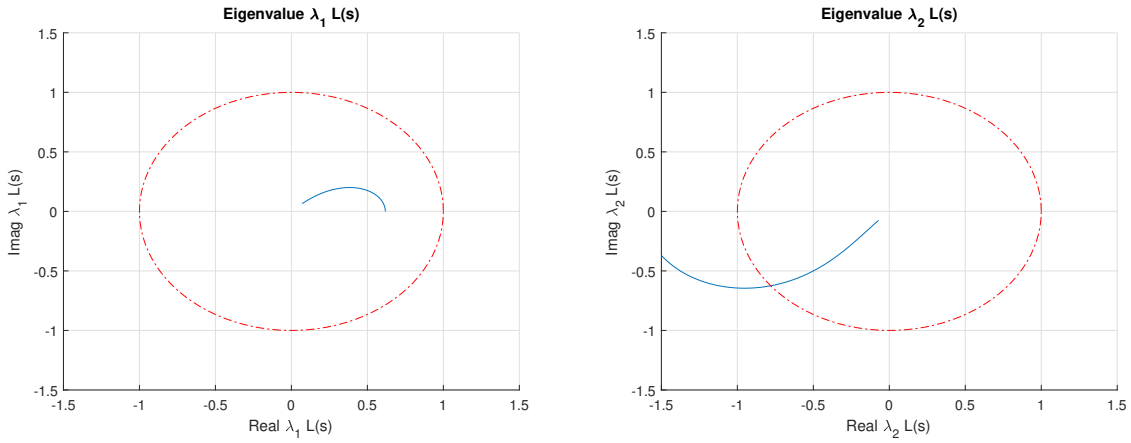

(a) λ_1 of L(s)

(b) λ_2 of L(s)

Figure 7.3: Eigenvalues of L(s)

the imaginary axis. However, they are not considered to RHP poles according to the nyquist theorem. Stability of a MIMO closed-loop can be determined characteristic loci. The loci should make P (number of RPH open loop poles) anti-clockwise encirclements, which is zero for this system. Furthermore, the loci can not pass trough the origin. The problem why this system seems to be stable has to do with one of the off diagonal terms being equal to zero. When a small delta is applied to the imaginairy poles the system does become stable for the closed loop.

8 Exercise 2.13

a) The state-space representation of a suspended two-mass-spring-damper system is given by equation 8.1. A system is called asymptotically stable when all eigenvalues of A are strictly negative. Therefore, the given system is asymptotically stable which implies stability.

$$G = \left[\begin{array}{c|c} A & B \\ \hline C & D \end{array}\right] = \left[\begin{array}{cccc|c} -\frac{d+d_s}{m} & -\frac{c+c_s}{m} & \frac{d}{m} & \frac{c}{m} & \frac{1}{m} \\ 1 & 0 & 0 & 0 & 0 \\ \frac{d}{m} & \frac{c}{m} & -\frac{d}{m} & -\frac{c}{m} & 0 \\ 0 & 0 & 1 & 0 & 0 \\ \hline 0 & 0 & 0 & 1 & 0 \end{array}\right] \tag{8.1}$$

The Hautus lemma can be used to check if a system is controllable $rank[\lambda I - A, B]$ remains full rank for $\lambda \in \mathbb{C}$. To check if a system is observable, the Hautus lemma $rank[\lambda I - A, C]$ remains full rank for $\lambda \in \mathbb{C}$. Our system only contains strictly negative eigenvalues and is therefore controllable and observable. The bode diagram of the system is given in figure, 8.1a.

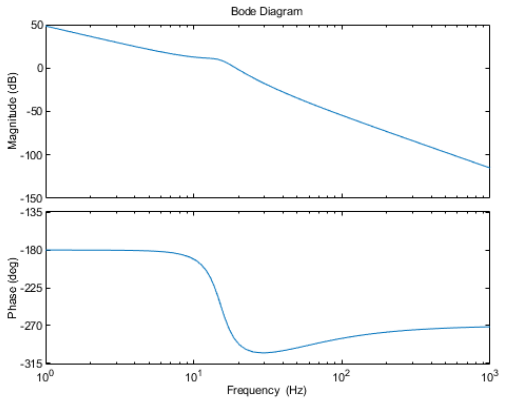

(a) Bode diagram of the plant G

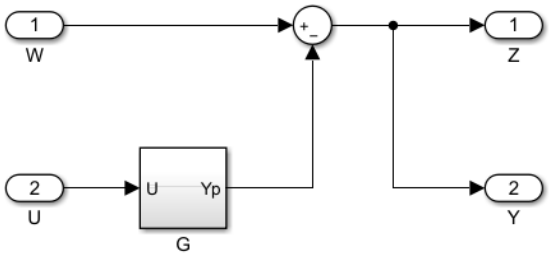

(b) Interior of P_1

Figure 8.1

b) The next step is to construct a standard plant. The given inputs and outputs of the standard plant are shown in equation 8.2. A graphical figure of the interior of P_1 is given by figure 8.1b.

$$\begin{aligned} y = e &= r - y_p \\ z &= r - y_p \end{aligned} \tag{8.2}$$

Where, $r = w$ and $y_p = u \cdot G$, substituting this in equation 8.2 leads to the following transfer matrix from $(w, u)^T$ to $(z, y)^T$, equation 8.3.

$$\begin{bmatrix} z \\ y \end{bmatrix} = \begin{bmatrix} I & -G \\ I & -G \end{bmatrix} \begin{bmatrix} w \\ u \end{bmatrix} \tag{8.3}$$

The closed loop transfer function from w to z is computed using $M = P_{11} + P_{12}K(I - P_{22}K)^{-1}P_{21}$. In this case this results in the sensitivity function, $\mathcal{F}_l(P_1, K) = I(I + GK)^{-1}$.

c) A minimal realization of P_1 is generated using MATLAB. First the transfer function of the previous exercises is used, equation 8.3. Next, a P_{1ss} is computed using a state space realization. P_{1ss} has the same transfer function as P_1. However, both of them can be usefull depending on the application. A transfer function is more usefull when system should be tuned. The state-space representation is better for system analysis (observability, stability, controlability) or solving H_∞ problems.

d) The *hinfsyn* MATLAB function is used to compute controller K_1. For γ a value of 1.0016 is achieved. The order of the controller is the equal to four, which is the same as the number of states of the original plant. Moreover, four is also the minimal order for the controller.
e) Using the *lft* function in MATLAB, the closed loop between P_1 and K_1 is computed. The bode diagram can be seen in figure 8.2a. The $\mathcal{H}_\infty$ norm for a SISO system is computed using $||\mathcal{S}(S)||_\infty = \sup|S(j\omega)|$, which is essentially the "worst case" frequency. The γ value is equal to 0.0138 dB, which is indeed equal to the worst case frequency in the bode of the closed loop function. The corresponding transfer function behaviour is equal to our expectations. According to the bode sensitivity integral the area below zero should equal the area above zero.

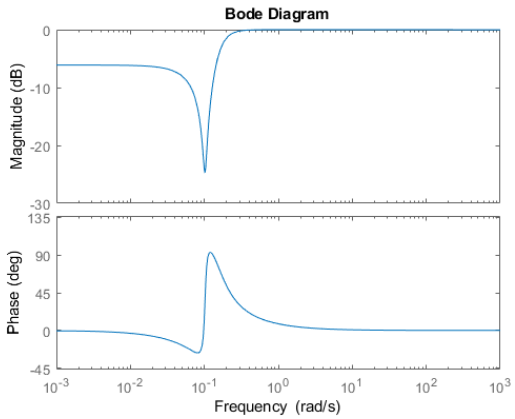

(a) Bode diagram of the closed loop

f) The weighting filter W2 is given as equation 8.4. Both the weighting filter and the inverse of the weighting filter are plotted in a bode diagram. As can be seen in figure 8.3.

$$W_2(s) = \frac{s^2 + 4\pi\beta f_{BW} s + (2\pi f_{BW})^2}{\left(s + 2\pi \frac{f_{BW}}{20}\right)^2} \tag{8.4}$$

g) A weighted standard plant should be created. The exogenous output z now becomes $W_2 e$, with $e = r - y_p$. The weighted standard plant is denoted as P_2 in equation 8.5.

$$\begin{bmatrix} z \\ y \end{bmatrix} = \begin{bmatrix} W_2 & -W_2 G \\ I & -G \end{bmatrix} \begin{bmatrix} w \\ u \end{bmatrix} \tag{8.5}$$

The closed loop transfer function from w to z is computed using $M = P_{11} + P_{12}K(I - P_{22}K)^{-1}P_{21}$. In this case this results in, $\mathcal{F}_l(P_2, K) = W_2(I + GK)^{-1}$.Furthermore, P_2 is

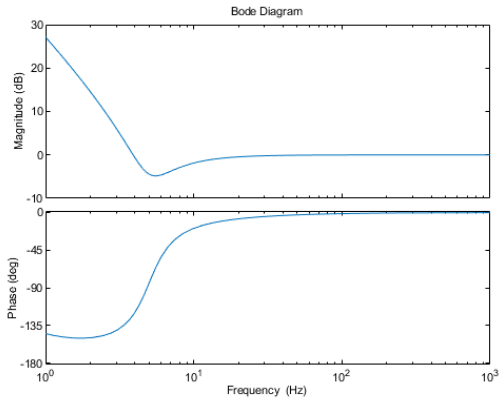

(a) Bode diagram of weight W2

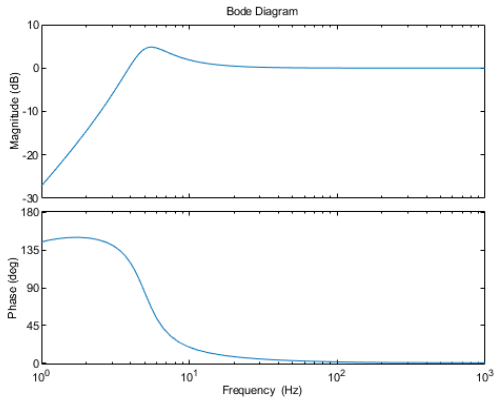

(b) Bode diagram of inverse weight W2

Figure 8.2

implemented in MATLAB, using the *augw* function. Which results in a 6th order system. Moreover, this is caused by the order of the plant(4) augmented with the order of the weighting filter(2).

h) If a controller is computed and $||\mathcal{F}_l(P_2, K_2)||_\infty$<1. There can be concluded that $|S_2(j\omega)|$ is succesfully bounded by $|\frac{1}{W_2(j\omega)}|$.

i) The controller K_2 is computed by minimizing $||\mathcal{F}_l(P_2, K_2)||_\infty$. The order of the resulting controllerK_2 is equal to 6, which is the same order as the weighted standard plant. The achieved γ is equal to 1.0016.

j) The bode magnitude plot is created for $\mathcal{F}_l(P_2, K_2)$. The figure 8.3a shows that the function is bounded by γ of the previous question.

k) A bode magnitude plot is created for $\mathcal{F}_l(P_1, K_2)$ and $1/W_2$. The figure can be found at 8.3b, as we expected the closed loop of the general plant is bounded by the weighing function.

l) A higher bandwidth can be enforced by increasing the f_{BW}. As can be seen in figure 8.4a. Therefore, the performance can be increased. Furthermore, the γ will increase as well.
m) $\gamma \approx 1$ can be obtained when f_{BW} decreases to $\omega \approx 0$. However, γ cannot become smaller then one because of the bode sensitivity integral.

n) Now a perturbed plant is introduced with a different spring constant. A step response is created by applying a step to the input r and measuring output e, for both the nominal plant and the perturbed plant. Furthermore, The performance filter with 5 Hz created the controller K_2. The performance filter with 20 Hz created the controller K_3. The step responses can be seen in figure 8.4a. As we expected the performance of the nominal controller increases when the increased performance filter K_3 is applied. However, for the perturbed plant the system becomes unstable.

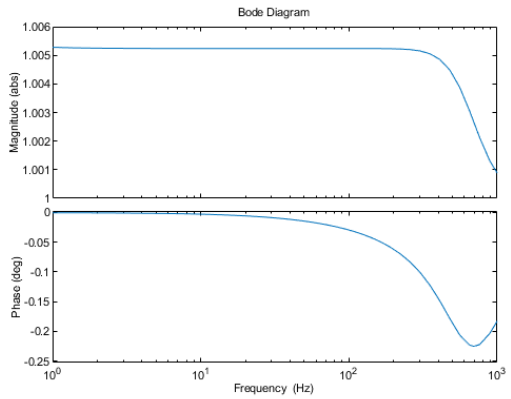

(a) Absolute bode magnitude plot $\mathcal{F}_l(P_2, K_2)$

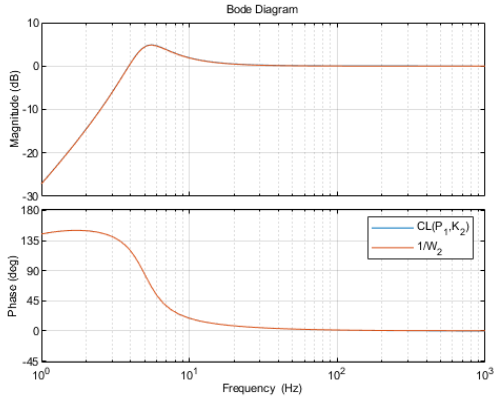

(b) Bode magnitude plot $\mathcal{F}_l(P_1, K_2)$

Figure 8.3

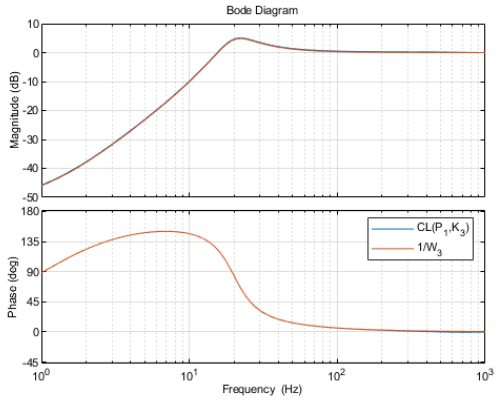

(a) Bode magnitude plot $\mathcal{F}_l(P_1, K_3)$

o) Now the *mixsyn* function from MATLAB is used to synthesize the controller. As an input to the function two weighting functions are used, the Wi weighting filter is used as a bound on the complementary sensitivity function, equation 8.7. The Wp weighting filter ensures the performance of the system described by equation, 8.6. The γ is computed by the *mixsyn* synthesize to be equal to 0.7370. The controller seems to be stable for both plants as can be seen in figure 8.5c, this is ensured by the weighting filter Wi. RP is achieved because the maximum singular value of N is smaller then 1, the maximum singular value of N is equal to gamma.

$$w_P(s) = \frac{1}{2}\frac{(s + 2\pi f_{BW})^2}{\left(s + 2\pi \frac{f_{BW}}{10}\right)^2} \tag{8.6}$$

$$w_I(s) = 2000\frac{s^2 + 2\beta_1\omega_1 s + \omega_1^2}{s^2 + 2\beta_2\omega_2 s + \omega_2^2} \tag{8.7}$$

p) To improve performance f_BW can be increased up to 9 Hz. After 9 Hz the maximum singular value is above 1 and therefore Robust Performance is not achieved.The values of the

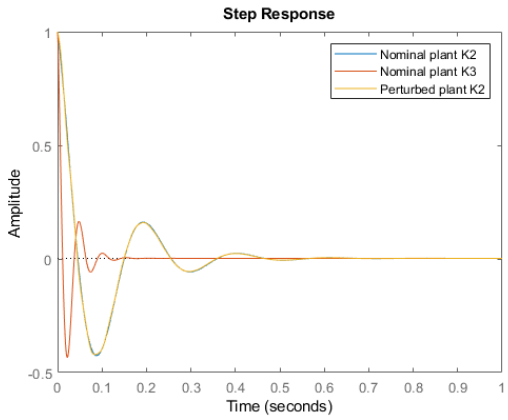

(a) Stable step responses

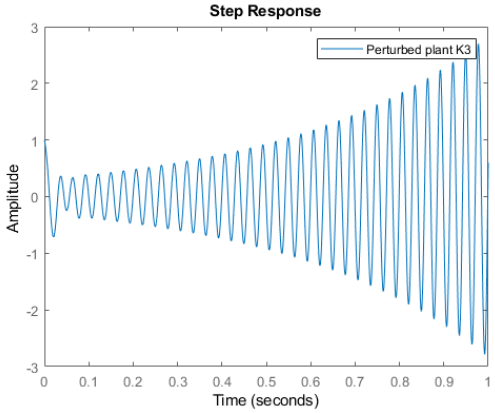

(b) Unstable step response

Figure 8.4: Step response of nominal and perturbed plant

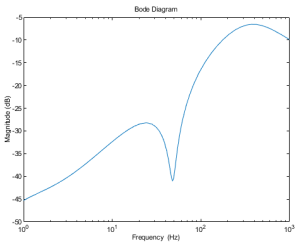

(a) Controller K_1

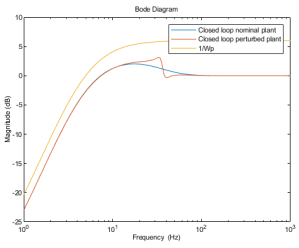

(b) Closed loop systems

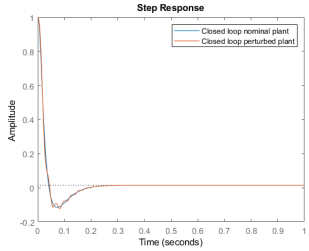

(c) Step responses of both plants

Figure 8.5: Mixsyn synthesize controller results

singular values can be seen in figure 8.6

q) To check if the resulting controller internally stabilizes the plant (4.8.1,lemma 4.8) is used. This lemma states that Q should be stable:

Lemma 4.8 *For a stable plant G(s) the negative feedback system is internally stable if and only if* $Q = K(I + GK)^{-1}$ *is stable.*

The plant should be stable in order to use this lemma. In exercise 13.a is determined that the plant is stable. Q is computed using MATLAB, furthermore the stability of Q is tested by the poles of the system. Q is stable because all the poles are strictly negative.

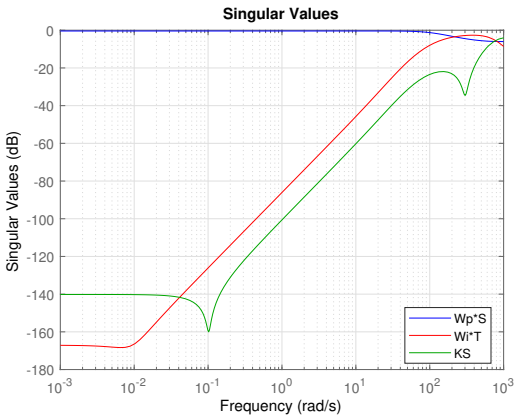

(a) Singular values N

Figure 8.6: Mixsyn synthesize controller results

9 Exercise 2.14

a) A relevant state-space model of a H-drive is given. In order to scale the transfer matrix to make proper performance specifications, first a matrix W_{sc} is applied. This matrix ensures that the output of the transfer matrix has the right units. To reach the required bandwidth of 50Hz another scaling matrix is applied. Therefore, the scaled plant is defined as $\tilde{G}(s) = W_{sc}G(s)V_{sc}$. To ensure the 0dB crossing is at our desired bandwidth the V_{sc} is chosen as:

$$V_{sc} = \begin{bmatrix} 10^5 & 0 \\ 0 & 10^{4.28} \end{bmatrix} \tag{9.1}$$

The bode figures of the original plant and the scaled plant can be found in figure 9.1.

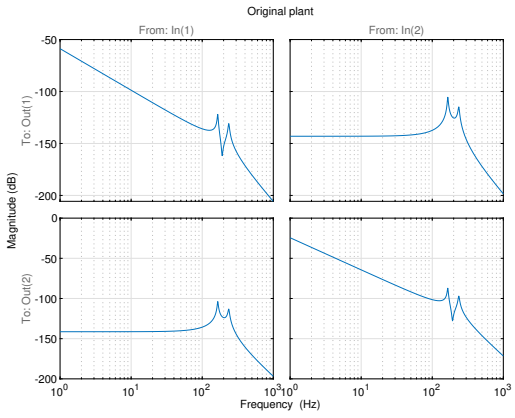

(a) Bode magnitude scaled plant

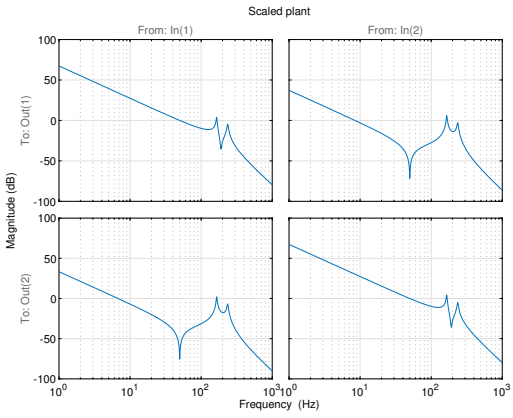

(b) Bode magnitude scaled plant

Figure 9.1: Bode magnitude plants

b) For the scaled plant of the previous question, now performance weights are defined. The scaled four block problem becomes as follows:

$$\tilde{M} = -\begin{bmatrix} W_1\tilde{S} & W_1\tilde{S}\tilde{G} \\ W_2\tilde{K}\tilde{S} & W_2\tilde{K}\tilde{S}\tilde{G} \end{bmatrix} = -[M_1 \quad M_2] \tag{9.2}$$

Furthermore, W_1 is chosen as equation 9.3. With $K_{S,1} = K_{S,2} = 0.5$ and $f_{i,1} = f_{i,2} = 5$. The weighting filter W_1 can be seen in figure 9.2a. The weighting filter acts as a bound on the sensitivity and process sensitivity. A $\mathcal{H}_\infty$-controller ensures that all entries become small. Therefore, a few design objectives are:

- M_2 dominant before bandwidth because controller is keeping $||\tilde{M}||_\infty$ small
- W_1 contains integrator action to force +20dB/dec slope on $|\tilde{S}\tilde{G}|$
- Suppression of 6dB after integral frequency f_i

$$W_1(s) = \begin{bmatrix} \frac{k_{S,1}(s+2\pi f_{i,1})}{s} & 0 \\ 0 & \frac{k_{S,2}(s+2\pi f_{i,2})}{s} \end{bmatrix} \tag{9.3}$$

c)W_2 is chosen as equation 9.4. With $K_{S,1} = K_{S,2} = 0.5$, $f_{r,1} = f_{r,2} = 500$ and $\alpha = 20$. The weighting filter W_2 can be seen in figure 9.2b.The weighting filter acts as a bound on the control sensitivity and complementary sensitivity. A $\mathcal{H}_\infty$-controller ensures that all entries become small. Furthermore, the design objectives of this filter are:

- W_2 dominant after bandwidth because controller is keeping $||\tilde{M}||_\infty$ small
- W_2 has a roll-off slope of -20dB/dec on $|\tilde{K}\tilde{S}|$
- Suppression of -6dB before roll-off frequency f_r

The purpose of parameter α is to ensure that the filter is proper. Therefore, an additional pole is added to the filter at a higher frequency. α determines at which distance the pole is located from the roll-off frequency f_r.

$$W_2(s) = \begin{bmatrix} \frac{k_{S,1}(s+2\pi f_{r,1})}{\frac{1}{\alpha}s+2\pi f_{r,1}} & 0 \\ 0 & \frac{k_{S,2\pi}(s+2\pi f_{r,2})}{\frac{1}{\alpha}s+2\pi f_{r,2}} \end{bmatrix} \tag{9.4}$$

d) M as in equation 9.5 is verified. The outputs can be derived from the inputs as follows. z_1 can be derived as equation 9.8 as follows:

$$\begin{bmatrix} z_1 \\ z_2 \end{bmatrix} = M \begin{bmatrix} w_1 \\ w_2 \end{bmatrix} \tag{9.5}$$

$$z_1 = -w_1 - w_2G - z_1KG \tag{9.6}$$

$$z_1(I + KG) = -w_1 - w_2G \tag{9.7}$$

$$z_1 = (-w_1 - w_2G)(I + KG)^{-1} \tag{9.8}$$

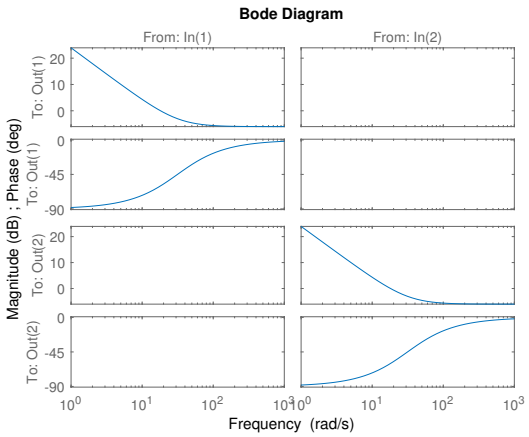

(a) Bode diagram of weighting filter W_1

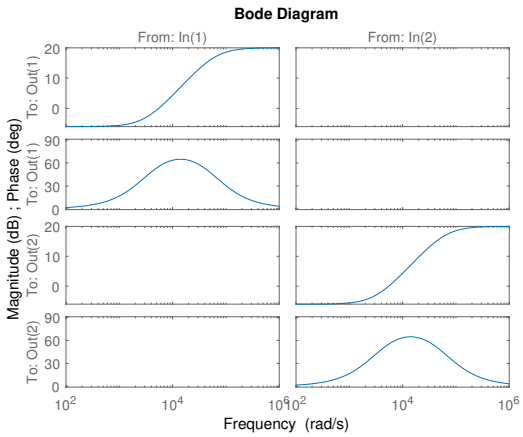

(b) Bode diagram of weighting filter W_2

Figure 9.2: Bode diagram of performance weights

z_2 can be derived as 9.11, see following steps:

$$z_2 = -w_1 - w_2GK - z_2KG \tag{9.9}$$

$$z_2(I + KG) = -w_1K - w_2KG \tag{9.10}$$

$$z_2 = (-w_1K - w_2GK)(I + KG)^{-1} \tag{9.11}$$

Combining both z_1, z_2 and $S = (I + KG)^{-1}$ in matrix from, M is obtainted:

$$M = -\begin{bmatrix} S & SG \\ KS & KSG \end{bmatrix} \tag{9.12}$$

e) A nominal plant $\overline{P}$ is defined as in equation 9.13. Furthermore, $\overline{P}$ determined with the unscaled plant G(s) and the signal flow.

$$\begin{bmatrix} z_1 \\ z_2 \\ y \end{bmatrix} = \overline{P} \begin{bmatrix} w_1 \\ w_2 \\ u \end{bmatrix} \tag{9.13}$$

The signals are determined as follows:

$$\begin{aligned} z_1 &= -w_1 - (w_2 + u)G \\ z_2 &= u \\ y &= -w_1 - (w_2 + u)G \end{aligned} \tag{9.14}$$

Combining those equations into a matrix form, $\overline{P}$ becomes:

$$\overline{P} = -\begin{bmatrix} -I & -G & -G \\ 0 & 0 & I \\ -I & -G & -G \end{bmatrix} \tag{9.15}$$

f) Why would it be preferable to use the state-space representation of $\overline{P}$? State-space can be easily writen in transfer function form. Furthermore, via state-space it is easier to compute some tests, such as controllablility and observability. Moreover, state-space is faster computationally in MATLAB because it uses matrices.

g) The scaled output sensitivity S_{sc} and the original sensitivity function S are related as follows:

$$\tilde{S} = W_{sc} S W_{sc}^{-1} \tag{9.16}$$

This equation is derived from $\tilde{G} = W_{sc} G V_{sc}$ and $K = V_{sc} \tilde{K} W_{sc}$. $\tilde{K}$ is defined as follows:

$$\tilde{K} = V_{sc}^{-1} K W_{sc}^{-1} \tag{9.17}$$

Now $\tilde{L}$ is defined as:

$$\tilde{L} = \tilde{G}\tilde{K} = W_{sc} G V_{sc} V_{sc}^{-1} K W_{sc}^{-1} = W_{sc} G K W_{sc}^{-1} \tag{9.18}$$

Therefore, $\tilde{S}$ is equal to:

$$\tilde{S} = \frac{I}{I + W_{sc} G K W_{sc}^{-1}} \tag{9.19}$$

Pre and post multiplying S with W_{sc} and W_{sc}^{-1} gives:

$$W_{sc} S W_{sc}^{-1} = \frac{(W_{sc} W_{sc}^{-1})}{(W_{sc} W_{sc}^{-1}) + W_{sc} G K W_{sc}^{-1}} = \tilde{S} \tag{9.20}$$

Furthermore, $\tilde{M}$ can now be expressed as WMV which is done in the following equations:

$$\tilde{M} = -\begin{bmatrix} W_1 \tilde{S} & W_1 \tilde{S} \tilde{G} \\ W_2 \tilde{K} \tilde{S} & W_2 \tilde{K} \tilde{S} \tilde{G} \end{bmatrix} \tag{9.21}$$

W and V can now be extracted from $\tilde{M}$ as follows:

$$\tilde{M} = -\begin{bmatrix} W_1 W_{sc} & 0 \\ 0 & W_2 V_{sc}^{-1} \end{bmatrix} \begin{bmatrix} S & SG \\ KS & KSG \end{bmatrix} \begin{bmatrix} W_{sc}^{-1} & 0 \\ 0 & V_{sc} \end{bmatrix} \tag{9.22}$$

h) The generalized plant P is used with the H_∞-control synthesize to create a controller. Are the results satisfactory? No, can not find a stabilizing controller.

i) -

j) When the poles are shifted away from the origin by a small number, the H_∞-control synthesize is able to find a suitable controller.

k) All control objectives satisfied? No, because the γ is equal to 1.6 which is lager then 1 and therefore exceeds at least one of the performance weights. The controller of the H_∞-control synthesis is given in 9.3. From the image can be concluded that the control synthesis used multiple notch filters around the resonance frequency to achieve the necessary performance. In figure 9.4 the $\tilde{M}$ of the system are plotted together with the corresponding weighting filter.

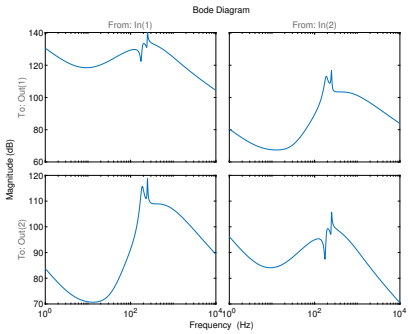

(a)

Figure 9.3: Bode diagrams of controller K

From here it can be seen that the controller tries to achieve the previous stated performances (14.b). However, K is not able to control the system as as indicated by γ.
l) To measure interaction in a system RGA can be used. The RGA of this plant is computed and plotted in figure 9.5a. If the RGA is equal to identity the system is perfectly decoupled and there is no interaction between states. This system is not perfectly decoupled because the RGA is not equal to identity around the resonant peaks. Furthermore, this is the case because the system is rigid body mode decoupled, therefore the flexible modes are still visible in the plant.
m) -

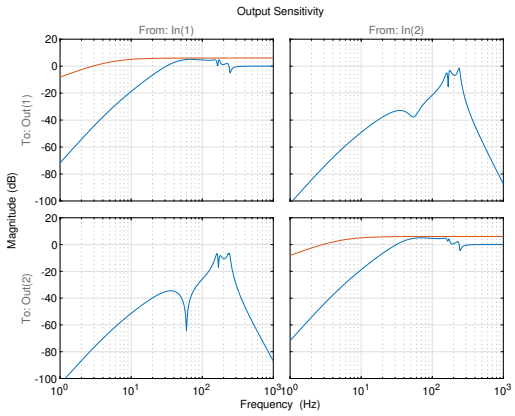

(a) Bode diagrams of Output Sensitivity

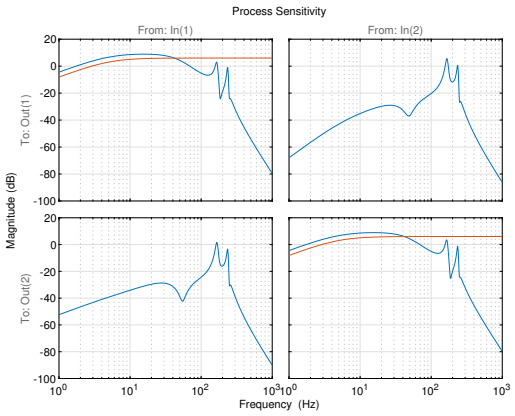

(b) Bode diagrams of Process Sensitivity

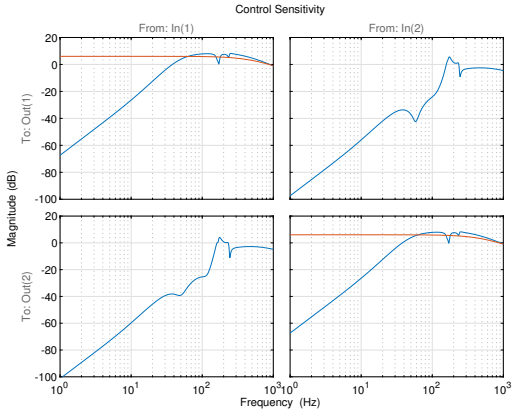

(c) Bode diagrams of Control Sensitivity

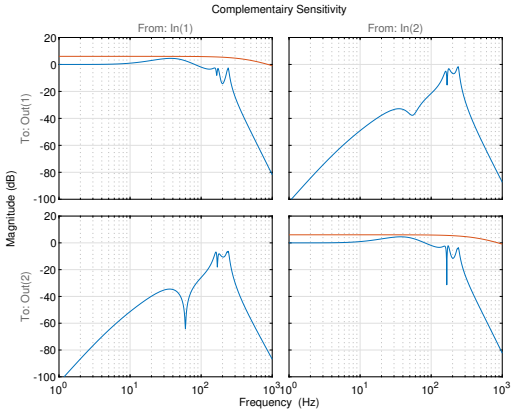

(d) Bode diagrams of Complementary Sensitivity

Figure 9.4: $\tilde{M}$ compared to performance filters

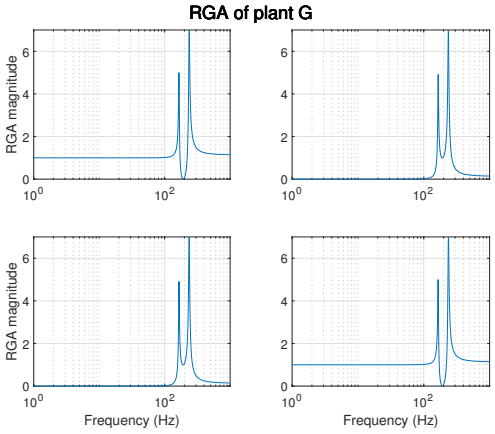

(a) Relative gain array plant